

Article

# Promising Prognosis Marker Candidates on the Status of Epithelial–Mesenchymal Transition and Glioma Stem Cells in Glioblastoma

Yasuo Takashima <sup>1</sup>, Atsushi Kawaguchi <sup>2</sup> and Ryuya Yamanaka <sup>1,\*</sup>

<sup>1</sup> Laboratory of Molecular Target Therapy for Cancer, Graduate School of Medical Science, Kyoto Prefectural University of Medicine, Kyoto 602-8566, Japan; ytakashi@koto.kpu-m.ac.jp

<sup>2</sup> Center for Comprehensive Community Medicine, Faculty of Medicine, Saga University, Saga 849-8501, Japan; akawa@cc.saga-u.ac.jp

\* Correspondence: ryaman@koto.kpu-m.ac.jp

Received: 29 September 2019; Accepted: 22 October 2019; Published: 24 October 2019



**Abstract:** Multivariable analyses of global expression profiling are valid indicators of the prognosis of various diseases including brain cancers. To identify the candidates for markers of prognosis of glioblastoma, we performed multivariable analyses on the status of epithelial (EPI)–mesenchymal (MES) transition (EMT), glioma (GLI) stem cells (GSCs), molecular target therapy (MTT), and potential glioma biomarkers (PGBs) using the expression data and clinical information from patients. Random forest survival and Cox proportional hazards regression analyses indicated significant variable values for *DSG3*, *CLDN1*, *CDH11*, *FN1*, *HDAC3/7*, *PTEN*, *L1CAM*, *OLIG2*, *TIMP4*, *IGFBP2*, and *GFAP*. The analyses also comprised prognosis prediction formulae that could distinguish between the survival curves of the glioblastoma patients. In addition to the genes mentioned above, *HDAC1*, *FLT1*, *EGFR*, *MGMT*, *PGF*, *STAT3*, *SIRT1*, and *GADD45A* constituted complex genetic interaction networks. The calculated status scores obtained by principal component analysis indicated that GLI genes covered the status of EPI, GSC, and MTT-related genes. Moreover, survival tree analyses indicated that  $MES^{high}$ ,  $MES^{high}GLI^{low}$ ,  $GSC^{high}GLI^{low}$ ,  $MES^{high}MTT^{low}$ , and  $PGB^{high}$  showed poor prognoses and  $MES^{middle}$ ,  $GSC^{low}$ , and  $PGB^{low}$  showed good prognoses, suggesting that enhanced EMT and GSC are associated with poor survival and that lower expression of EPI markers and the pre-stages of EMT are relatively less malignant in glioblastoma. These results demonstrate that the assessment of EMT and GSC enables the prediction of the prognosis of glioblastoma that would help develop novel therapeutics and de novo marker candidates for the prognoses of glioblastoma.

**Keywords:** glioblastoma; glioma stem cell; epithelial-mesenchymal transition; multivariable analysis; prognosis prediction

## 1. Introduction

The World Health Organization (WHO) classifies gliomas into four categories based on malignancy and overall survival (OS) [1]. Glioblastoma is the most malignant form of astrocytoma that is fast-growing (grade 4 glioma) [1,2]. The median OS of glioblastoma is 9–15 months and the five-year survival rate remains less than 5% [1,3–5]. Radiotherapy with six cycles of concomitant temozolomide, an oral alkylating agent with minimal additional toxicity, is the standard treatment after surgery in glioblastoma patients [2,4,5]. Thus, there is an immediate requirement for the early diagnosis and precise prediction of the prognosis for treatments of glioblastoma.

The invasiveness of glioblastoma depends on its high infiltration potential to invade the basement membranes of surrounding tissues [6–9]. Glioma cells are reprogrammed to have increased motility via weakened cell adhesions and a dysregulated cytoskeleton; this is known as epithelial–mesenchymal

transition (EMT) [10]. EMT is a biological process that polarized epithelial cell sheets undergo, wherein multiple biochemical changes culminate in mesenchymal phenotypes [6]. Cells display altered morphology, resistance to chemotherapy, and *anoikis* (a form of programmed cell death of cells detached from the basement membranes) [11,12]. EMT is also involved in other biological processes, including implantation and embryo development, wound healing, tissue regeneration, and neoplasia associated with cancer progression [12]. During invasion in cancer, phenotypes also change as EMT is mainly induced by hypoxia and the transforming growth factor (TGF)- $\beta$  released from glioma stem cells (GSCs), mesenchymal stem cells (MSCs), and myeloid cells recruited by hypoxia [13]. The reverse is also essential for the formation of distant or disseminated tumor nodules [10].

Stem cells, including cancer stem cells (CSCs), are pluripotent and capable of self-renewal, like induced pluripotent stem (iPS) cells induced by the transcription factors Oct3/4, Sox2, c-Myc, and Klf4 [14] or OCT4, SOX2, NANOG, and LIN28 [15]. The expression of OCT4, MYC, and KLF4 increases with increasing malignancy in astrocytomas, whereas MYC expression slightly decreases in recurrent glioblastomas [16]. Exposure to temozolomide (TMZ) increases the expression of KLF4 and reduces the expression of Nanog and OCT4 in glioma cells [16], indicating that stem cell factors, especially KLF4, play pivotal roles in GSCs. The most common GSC marker CD133, also known as prominin-1 (*PROM1*), is used to isolate GSCs by fluorescence-activated cell sorting (FACS) in primary glioma tissues and the cell lines U87 and T98G [17]. There are changes in metabolism in glioma and oxidative phosphorylation, glycolysis, and glutaminolysis replace redox balance, bioenergetics, and biosynthesis, respectively [18]. Tumor progression is enhanced by inflammation, which is an emerging hallmark of cancers that depends on the balance of glioma cell proliferation, migration, and escape from the immune system [18]. However, the correlation between EMT and GSCs in glioblastoma has not been reported to date.

In this study, we focused on EMT and GSCs and performed multivariable analyses using the expression data and OS in patients with glioblastoma. To determine the distribution of survival of glioblastoma patients, we composed prognosis prediction formulae for the following components: epithelium (EPI), mesenchyme (MES), glioma (GLI), GSC, molecular target therapy (MTT) genes, and potential glioma biomarkers (PGBs). Consequently, several candidate genes were identified as promising glioblastoma predictors.

## 2. Materials and Methods

### 2.1. Data Set

Expression data and clinical information of patients with glioblastoma deposited in The Cancer Genome Atlas (TCGA) and the Chinese Glioma Genome Atlas (CGGA) were used [19,20]. Gene expression values of fragments per kilobase of exon per million reads mapped (FPKM) were normalized and subjected to the following analyses. The analyses were performed on the TCGA data set (151 samples) and the results were validated using the CGGA data set (135 samples) (Table S1). Tumor specimens were collected from untreated patients during surgery.

### 2.2. Gene Annotation

Genes of interest were annotated online at GOstat2.5 (<http://gostat.wehi.edu.au/>) [21] and Database for Annotation, Visualization, and Integrated Discovery (DAVID)6.8 (<https://david.ncifcrf.gov/>) [22].

### 2.3. Clustering Analysis

Gene expression values were modified with the variances from the means of patients, followed by hierarchical clustering analysis with the Ward method using the JMP built-in module (SAS Institute Inc., Tokyo, Japan). Heat maps were drawn to visualize their expression with a color configuration with red as high and green as low [23].

#### 2.4. Random Survival Forests Analysis

Random survival forests analysis was performed to determine the variable importance factors distinguishing gene expression associated with patient survival using the randomForestSRC package in R [24–26]. The variable importance values reflected the relative contribution of each variable to the prediction for the survival time, which was estimated by randomly permuting the values and recalculating the predictive accuracy of the model.

#### 2.5. Cox Hazards Regression Analysis

Correlations between gene expression and survival times were evaluated by the Cox proportional hazards regression analysis using the JMP built-in module (SAS Institute Inc.) [25,27].

#### 2.6. Survival Analysis

The Kaplan–Meier analysis was performed to estimate the survival distributions of subgroups with the log-rank test using the JMP built-in module (SAS Institute Inc.). The hazard ratio (HR) and confidence interval (CI) were calculated with a logistic regression model according to patients' survival times, which were assessed with a stepwise selection to compare the subgroups. Overall survival (OS) was defined as the date of diagnosis of glioblastoma to the date of death or last follow-up [19,20].

#### 2.7. Graphical Lasso Estimation

Genetic interactions with hub networks among variables from gene expression were analyzed by the graphical lasso estimation of Gaussian graphical models, such as a sparse inverse covariance matrix using a lasso (L1) penalty, using the glasso package in R [28,29].

#### 2.8. Principal Component Analysis (PCA)

Score correlation analysis was performed with formulae constituted by the first principal components derived from PCA. PCA was performed with the normalized FPKM values using the JMP built-in module (SAS Institute Inc.), which was used to classify the patients into the subgroups to estimate their prognoses in simple forms as linear combinations of expression values of the genes of interest [26].

#### 2.9. Survival Tree Analysis

Tree-structured survivals were analyzed to identify the largest differences in the Kaplan–Meier survival curves by dividing the patients into the most appropriate subgroups, harboring variable spaces as overall survival and interval censoring according to a constant model of the response variable in each partition [30]. The survival tree analysis was performed using the rpart package in R [31].

#### 2.10. Statistics

Statistical analyses were performed using R [32], Bioconductor [33], JMP10 (SAS Institute Inc.), and Microsoft Excel (Microsoft Corporation).  $p < 0.05$  was considered statistically significant.

### 3. Results

#### 3.1. Status of EMT and GSC Gene Expression in Glioblastoma

The aim of this study is to identify promising prognosis marker candidates of glioblastoma. As glioma is caused by EMT and maintained by glioma stem cells, in this study, we used the expression data and clinical information from 286 glioblastoma patients from TCGA and CGGA (Table S1) and focused on representative genes involved in EMT and glioma (Figure 1, Table S2) [34–37]. Expression of the 126 genes in 151 samples from the TCGA data set was shown with hierarchical clusters represented by heatmaps, including those in EPI (14 genes; Figure 1a), MES (23 genes; Figure 1b), GLI (53 genes;

Figure 1c), GSCs (17 genes; Figure 1d), MTT (34 genes; Figure 1e), and PGBs (24 genes; Figure 1f). However, distinct expression patterns capable of stratifying the patients into clusters were not identified, suggesting a possibility that differential expression of the genes requires combinations to evaluate the prognoses of glioblastoma patients. Thus, we tested whether combinations of the genes were associated with EMT and GSC in glioblastoma.

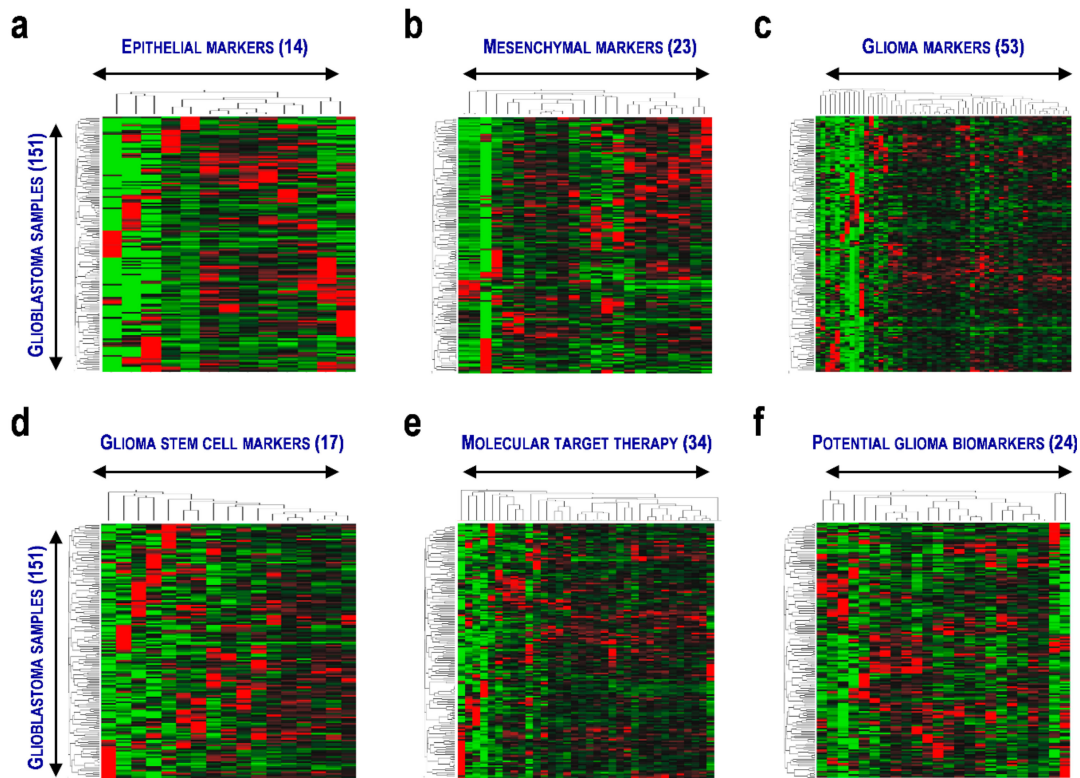


**Figure 1.** Differential expression of the genes related to epithelial–mesenchymal transition and glioma in 151 patients with glioblastoma. Expression patterns with two-way clustering analysis are presented. (a) Epithelial marker gene set. (b) Mesenchymal marker gene set. (c) Glioma marker gene set. (d) Glioma stem cell marker gene set. (e) Molecular target therapy gene set. (f) Potential glioma marker gene set. Numbers in the parentheses denote the numbers of genes and glioblastoma samples.

### 3.2. Importance of Significant Variables and Hazard Ratios of the Genes

Random survival forest analysis indicated the variable importance of each gene and the Cox proportional hazards regression analysis showed significant coefficient and hazard ratios (HRs) (Figure S1). A high variable associated with a significant coefficient and HR was seen in the following: *DSG3* and *CLDN1* as EPI markers (Figure S1a); *CDH11* and *FN1* as MES markers (Figure S1b); *FLT1*, *HDAC3/7*, and *PTEN* as GLI markers (Figure S1c); *L1CAM*, *OLIG2*, *BMI3*, and *STAT3* as GSC markers (Figure S1d); *EGFR*, *HDAC1/3/7*, and *SIRT1* as MTT genes (Figure S1e); and *TIMP4*, *IGFBP2*, *GFAP*, *GADD45A*, *MMP9*, and *MGMT* as PGBs (Figure S1f). Increased expression of *DSG3* (HR 1.36, 95% confidence interval (CI) 1.11–1.67,  $p = 0.004$ ), *FN1* (HR 1.29, 95% CI 1.08–1.56,  $p = 0.006$ ), *IGFBP2* (HR 1.18, 95% CI 1.04–1.35,  $p = 0.011$ ), *CLDN1* (HR 1.24, 95% CI 1.05–1.46,  $p = 0.013$ ), *HDAC7* (HR 1.36, 95% CI 1.04–1.77,  $p = 0.023$ ), and *L1CAM* (HR 1.10, 95% CI 1.01–1.19,  $p = 0.024$ ) were associated with poor prognoses of glioblastoma (Figure S2a–f). In contrast, an increased expression of *TIMP4* was associated with good prognosis of glioblastoma (HR 0.88, 95% CI 0.79–0.98,  $p = 0.025$ ; Figure S2g). An increase in *MGMT* and *MMP9* levels showed slightly poor prognoses of glioblastoma ( $p > 0.05$ ) (Figure S2h,i).

### 3.3. Evaluation of the Formulae for the Prediction of Prognosis of Glioblastoma

To determine patient survival, formulae were composed for 22 genes (Table S3) in a simple linear form using the sum of the integration of the coefficients and fragments per kilobase of exon per million mapped fragments (FPKM) of the normalized genes (Appendix A). Glioblastoma patients were divided into two subgroups based on the median status scores using the formulae. Subsequently, Kaplan–Meier survival curves were plotted (Figure 2). All of the low score subgroups showed good prognoses such as EPI<sup>low</sup> (HR 0.51, 95% CI 0.32–0.81,  $p = 0.0039$ ; Figure 2a), MES<sup>low</sup> (HR 0.41, 95% CI 0.27–0.62,  $p = 1.4 \times 10^{-5}$ ; Figure 2b), GLI<sup>low</sup> (HR 0.27, 95% CI 0.17–0.42,  $p = 1.6 \times 10^{-9}$ ; Figure 2c), GSC<sup>low</sup> (HR 0.34, 95% CI 0.21–0.55,  $p = 3.4 \times 10^{-6}$ ; Figure 2d), MTT<sup>low</sup> (HR 0.31, 95% CI 0.19–0.51,  $p = 1.5 \times 10^{-6}$ ; Figure 2e), and PGB<sup>low</sup> (HR 0.29, 95% CI 0.18–0.48,  $p = 2.7 \times 10^{-7}$ ; Figure 2f). The CGGA data set also showed similar results, although significances were not detected (Figure S3). These results indicate that the prognosis prediction formulae are useful to evaluate survival in glioblastoma patients. These formulae were associated with strong HRs for the GLI markers (HR 3.70), MTT genes (HR 3.22), and PGBs (HR 3.44), suggesting the success of the formulae. Gene ontology (GO) analysis (Table S4) indicated the gene sets that were associated with biological processes including proliferation (GO 0008284;  $p = 3.74 \times 10^{-7}$ ), metabolic process (GO 0051246;  $p = 8.02 \times 10^{-6}$ ), cell differentiation (GO 0030154;  $p = 4.81 \times 10^{-5}$ ), migration (GO 0030334;  $p = 7.58 \times 10^{-5}$ ), and histone H3 deacetylation (GO 0070932;  $p = 1.02 \times 10^{-4}$ ). These results suggest that the genes used for constructing the prognosis prediction formulae are involved in cancer development and progression.

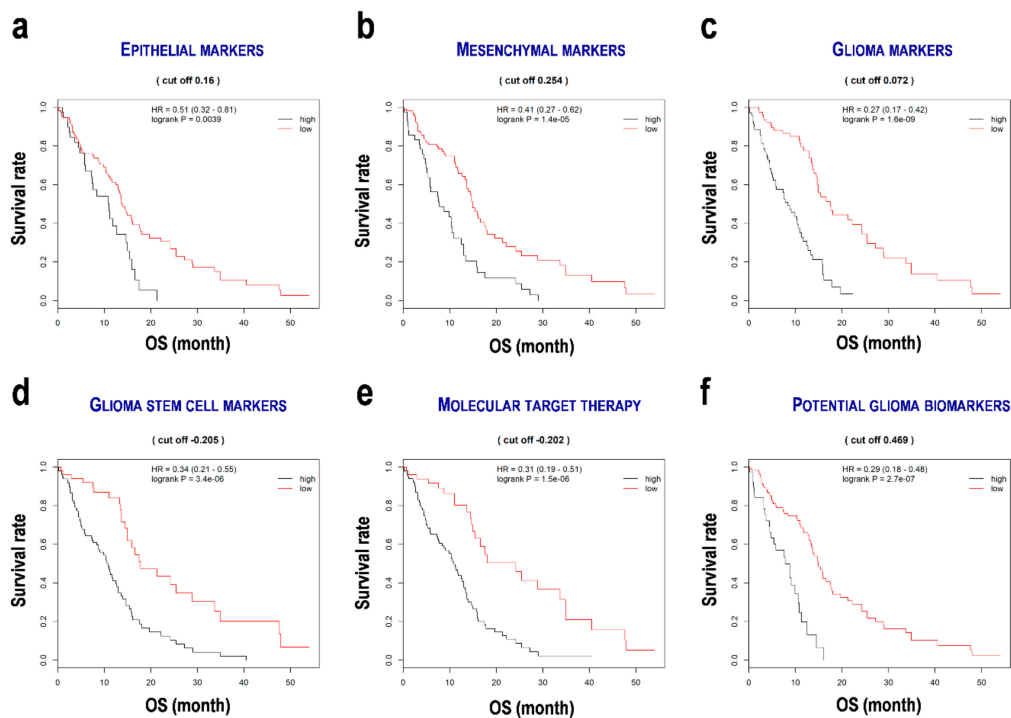


**Figure 2.** Survival distribution of the subgroups divided by the prognosis prediction formulae in the gene sets in glioblastoma. (a) Epithelial marker set. (b) Mesenchymal marker gene set. (c) Glioma marker gene set. (d) Glioma stem cell marker gene set. (e) Molecular target therapy gene set. (f) Potential glioma marker gene set. OS, overall survival; HR, hazard ratio; cut off score, a median score from a prognosis prediction formula. High and low denote the subgroups of the patients associated with the over and under median scores of the prognosis scores.

### 3.4. Genetic Interaction and Network Hubs within the Genes of Interest

We examined the genetic interactions based on the expression intensities to detect the network hubs and central factors in glioblastoma (Figure 3). The rates of composition of interacting to entry



prognosis of glioblastoma. However, combining GLI with markers of GSCs, MTT genes, and PGBs may enable the development of novel therapeutics and de novo candidate gene markers for predicting the prognosis of glioblastoma.

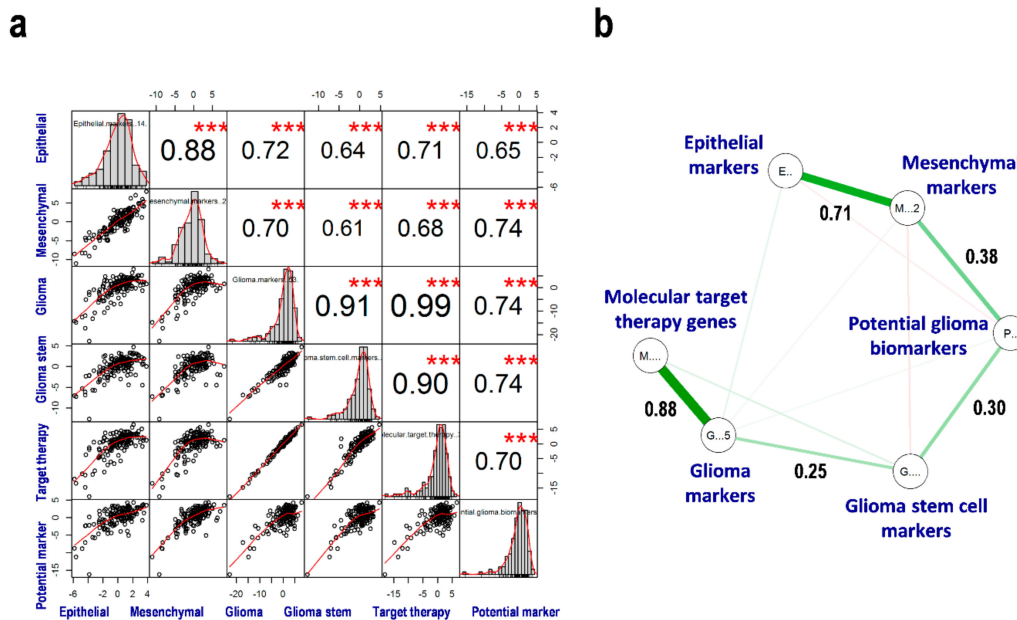


**Figure 4.** Correlation among the gene sets in glioblastoma. (a) Score correlation in glioblastoma. (b) The graphical lasso estimation with the network model of the gene sets related to epithelial–mesenchymal transition and glioma in glioblastoma. \*\*\*  $p < 0.0001$ .

### 3.6. Assessment using a Combination of EMT and GSCs in the Progression of Glioma

We tested some combinations of EMT and GSC relative to the OS of glioblastoma patients using survival tree analysis (Figure 5). Using the MES and GLI markers,  $MES^{middle}$  and  $MES^{low}GLI^{high}$  showed good prognoses, whereas  $MES^{high}GLI^{low}$  showed a poor prognosis (Figure 5a), suggesting that the expression of mesenchymal genes could be a good indicator for a prognosis of glioblastoma.  $MES^{middle}$  showed a stronger prognosis than  $MES^{high}$  (Figure 5b). Using the GLI and GSC markers,  $GSC^{low}$  showed a good prognosis, whereas  $GSC^{high}GLI^{low}$  showed a poor prognosis as compared with  $GSC^{high}GLI^{high}$  (Figure 5c), suggesting that GSC markers indicate malignant glioma cells. Moreover,  $PGB^{high}$  and  $PGB^{middle}$  showed poor prognoses as compared with  $PGB^{low}$  (Figure 5d,e), thereby validating the candidate markers and formulae used in this study.  $MES^{high}MTT^{low}$  showed a weaker prognosis than  $MES^{middle}$  and  $MES^{high}MTT^{high}$  (Figure 5f). This suggests that reduced expression of the target genes for MTT leads to poor patient survival. In contrast, the CGGA validation data set returned that  $EPI^{low}$  led to a better prognosis than  $EPI^{middle}$  and  $EPI^{high}$  (Figure S6a,b), suggesting a possibility that the overexpression of EPI genes can distinguish between the initiation of tumorigenesis and normal epithelial differentiation. Important data about GSC markers, MES markers, and PGBs could not be obtained from the CGGA data set (Figure S6c,d). Summarizing these results, the expression of EMT markers including MES, EPI, GSC, and PGBs could indicate a poor prognosis and malignant glioblastoma. Combinations of MES, GLI, and MTT gene markers might be useful for determining the prognosis of glioblastoma.

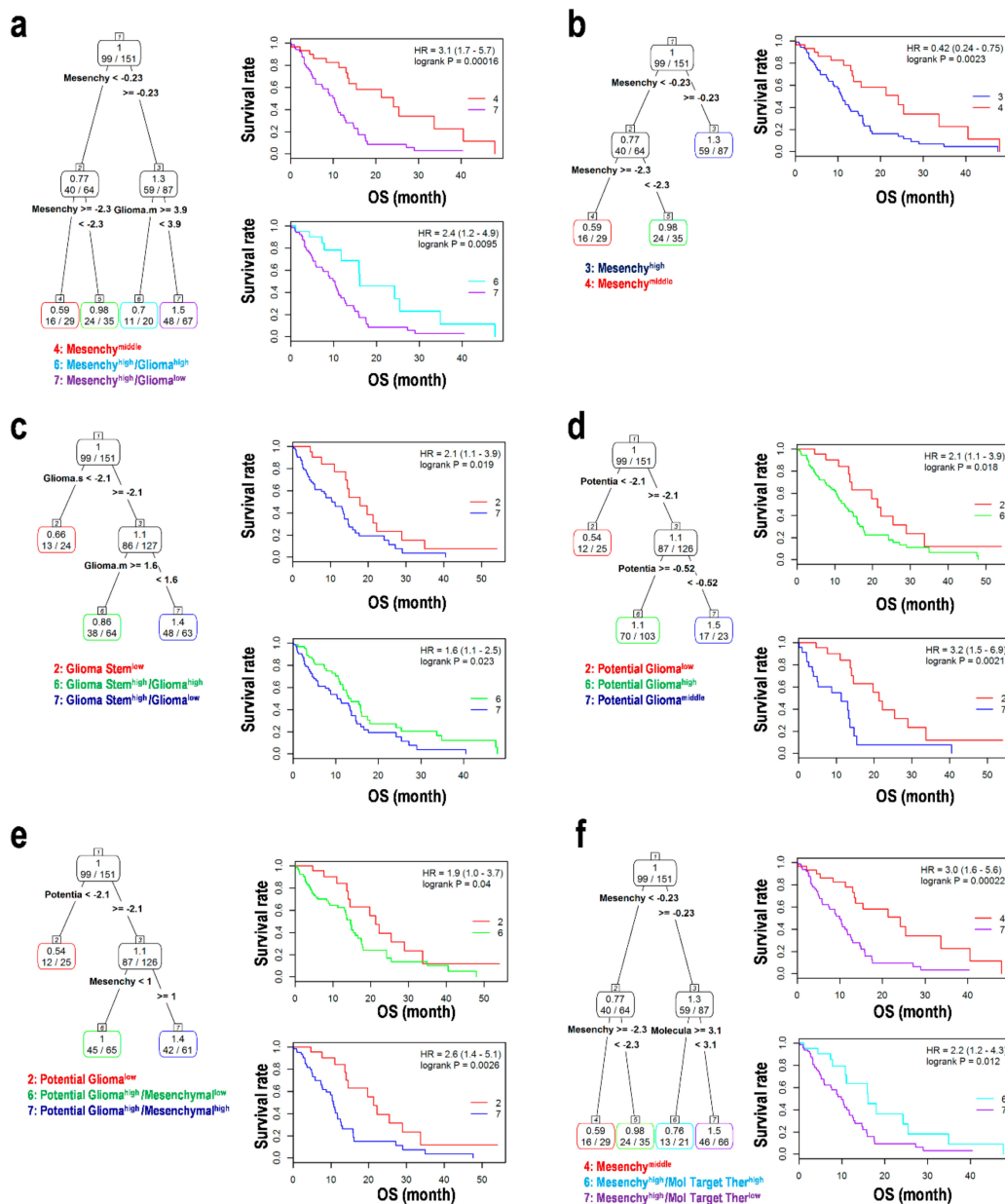


**Figure 5.** Survival tree analysis for the epithelial–mesenchymal transition (EMT) statuses and glioma markers in glioblastoma. (a) Mesenchymal status and glioma markers. (b) Mesenchymal status. (c) Glioma stem cell markers and glioma markers. (d) Potential glioma biomarkers. (e) Potential glioma biomarkers and mesenchymal status. (f) Mesenchymal status and molecular target therapy genes. HR; hazard ratio, OS; overall survival.

### 3.7. Multiple Assessments Required for Diagnosis and Predicting Prognosis of Glioblastoma

A combined formula was constituted based on the Cox proportional hazards regression analysis and our previous results (Appendix C). The formula distinguished the Kaplan–Meier survival curves of the subgroups divided by the median scores with a significant HR of 3.08 (95% CI 2.04–4.70,  $p < 0.0001$ ; Figure 6a) and the validation data set with similar results, but were not statistically significant (Figure 6b). To determine the important factors in the prognosis prediction formula based on representative genes like ESI, MES, GLI/GSC markers, and PGBs, we split the formulae used previously into several equations minus various factors (Figure 6c). Interestingly, the formulae without the GSC ( $\Delta$ GSC) and MES markers ( $\Delta$ MES) showed the opposite results in the risk ratio compared

with the normal combined formula (COMMON) in both the TCGA and CGGA data sets (Figure 6d,e), suggesting that evaluating MES and GSC markers is indispensable for the combined formula. The formulae missing EPI ( $\Delta$ EPI,  $\Delta$ EPI $\Delta$ GSC, and  $\Delta$ EPI $\Delta$ PGB) and GLI markers ( $\Delta$ GLI,  $\Delta$ GLI $\Delta$ GSC, and  $\Delta$ GLI $\Delta$ PGB) also weakened and/or reversed the risk ratios as compared with COMMON in both data sets (Figure 6d,e). Thus, the appropriate combination of several factors chosen based on the progression of glioma guarantees predicting the prognosis of glioblastoma.

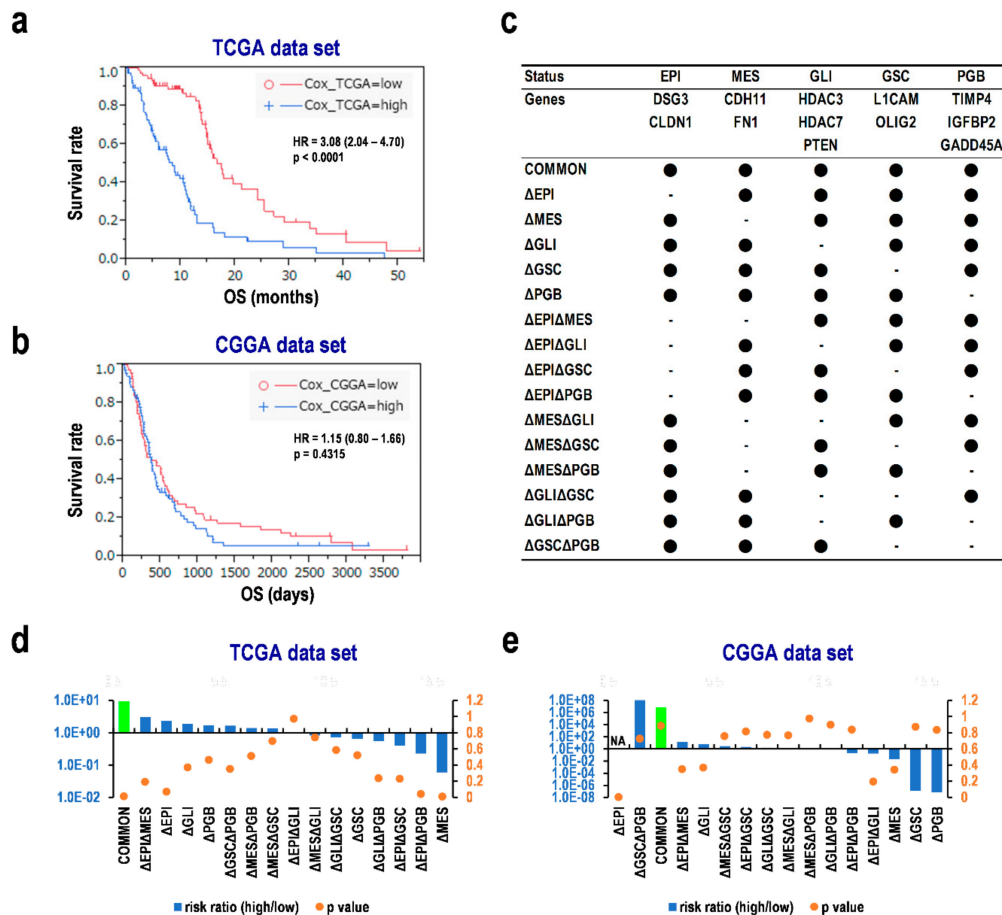


**Figure 6.** Contributions of EMT status and glioma stem cell markers for prognosis prediction in glioblastoma. (a–b) Survival distribution estimated with the combinatorial equation for prognosis prediction. (a) The Cancer Genome Atlas (TCGA) data set. (b) The Chinese Glioma Genome Atlas (CGGA) data set. Subgroups were divided by the median score from the formula in the data set. (c) The formula composition. (d–e) The risk ratios and *p*-values in the subgroups with a high score compared with those with a low score. (d) The TCGA data set. (e) The CGGA data set. EPI, epithelial status; MES, mesenchymal status; GLI, glioma markers; GSC, glioma stem cell markers; PGB, potential glioma biomarkers; NA, not applicable; HR, hazard ratio. Delta ( $\Delta$ ) represents a difference value.

## 4. Discussion

### 4.1. EMT and CSCs in Cancer Development and Progression

Cancer progression involves the induction of genetic stress and EMT, followed by CSC self-renewal, proliferation, and infiltration [38–40]. This process is also enhanced by the tumor microenvironment during angiogenesis and evasion of immune response and tumor cell properties, such as proliferation, migration, invasion, and drug resistance [38,40,41]. In glioma, chemo- and radiation-resistant GSCs have properties such as self-renewal and survival that contribute to tumor vasculature by transdifferentiating into endothelial cells upon induction with vascular endothelial growth factors

(VEGFs) and hepatoma-derived growth factors (HDGFs) [38]. EMT is associated with infiltration as well as the generation and maintenance of CSCs [39]. EMT also contributes to tumor invasion, heterogeneity, chemoresistance, and robustness in reprogrammed gene expression that enables morphological and functional dedifferentiation into CSCs from differentiated tumor cells [39]. Dysregulation of splicing factors and tumor-specific isoforms frequently occurs in human tumors, indicating the importance of post-transcriptional regulation, including alternative splicing and/or gene fusion [38,42,43]. Thus, it is considered that EMT and stem cell differentiation, including dedifferentiation into CSCs, are closely related to cancer development and progression. Therefore, cellular processes and intrinsic alterations such as alternative splicing would provide the base for developing novel chemical therapeutics and de novo therapies against cancers [27].

#### 4.2. Status Assessment and Prognosis Prediction using Multivariable Analyses on Gene Expression Profiling

Increased expression of *PD-L1* correlates with a poor outcome of glioblastoma [44]. Profiling of *PD-L1* expression is useful for determining patient survival time in glioblastoma [19,45]. A lower expression of type 2 T helper (Th2) cell genes compared with Th1 cell genes shows a good prognosis associated with lower expression of *PD-L1* and *PD-1* in glioblastoma, although estimating prognosis based on *PD-L1* and *PD-1* expression is difficult [19]. In the Th2<sup>low</sup> subgroup of patients with glioblastoma, a reduced expression of solute carrier family 11 (proton-coupled divalent metal ion transporter), member 1 (*SLC11A1*; encoding natural resistance-associated macrophage protein), tumor necrosis factor (TNF) receptor superfamily member 1B (*TNFRSF1B*), and lymphotoxin  $\beta$  receptor (*LTBR*) also show good prognoses [19,46]. TMZ is commonly used for treating glioblastoma and its mechanism of action is well known; however, the side effects associated are largely unknown [47,48]. The TMZ-stimulated glioblastoma cells suppress the expression of pro-inflammatory cytokines in activated periphery blood mononuclear cells. This depends on the enhanced expression of *PD-L1*, but no other immune checkpoint genes, such as *B7-H3*, herpesvirus entry mediator (*HVEM*), and galectin-9 (*LGALS9*), suggesting that TMZ controls the expression of *PD-L1* in glioblastoma cells, resulting in the evasion of the immune system [41]. An increased expression of *B7-H3* and the gene signature comprising *GATA3* and galectin-3 (*LGALS3*) show poor prognoses of glioblastoma [20], suggesting the involvement of the lectin family and oligosaccharide-mediated cell–cell and cell–matrix interactions on the antigen-presenting cell surface in their efficiency to understand glioblastoma progression as well as brain lymphoma [49,50]. Prediction of prognosis based on analyzing cellular processes is applicable to various tumors including other brain tumors, such as primary central nervous system lymphoma (PCNSL). The *PD-L1* protein is expressed in tumor microenvironments in 52% of cases, such as immune cells and macrophages. Patients with PCNSL (4.1%) also exhibit a rare and aggressive form of extra-nodal non-Hodgkin's lymphoma [51,52]. This indicates that *PD-L1* expression is detected in the surrounding and tumor cells. Thus, the assessment of cellular processes and prediction of prognosis with statistics from expression data are possible. Differential expression of *PD-1* and *PD-L2* and the Th1/Th2 balance enables the prediction of prognoses of PCNSL [27]. The formula comprising miR-30d, miR-93, and miR-181b is a promising marker for the prognosis of PCNSL [53]. The approaches and methods used in such studies could be applied to various diseases including brain tumors in assessing EMT and CSCs in this study. In addition, the candidates for diagnostic markers may also be detected from comparing with normal brain data.

## 5. Conclusions

In this study, we demonstrated that selective gene marker sets comprising 22 genes (Appendix A), such as *DSG3*, *FN1*, *IGFBP2*, *CLDN1*, *HDAC7*, and *L1CAM* as single gene marker candidates, are useful for predicting the prognosis of glioblastoma, based on the status assessment of EMT and GSCs that can be developed as novel target candidates for therapeutic intervention. The prognosis prediction formulae that included 12 genes (Appendix C), within a mixture of cellular processes, is effective in

evaluating the survival of glioblastoma patients, which would help develop novel therapeutics and provide de novo marker candidates to predict the prognosis of glioblastoma.

**Supplementary Materials:** The supplementary materials are available online at <http://www.mdpi.com/2073-4409/8/11/1312/s1>.

**Author Contributions:** Y.T. and R.Y. designed the study. Y.T. and A.K. performed experiments. Y.T., A.K., and R.Y. analyzed data. Y.T. and R.Y. wrote the manuscript.

**Funding:** This research was funded by the MEXT KAKENHI Grant Numbers 16H05441 (R.Y.) and 18K09001 (Y.T.).

**Conflicts of Interest:** The authors declare no conflict of interest. The funders had no role in the design of the study; in the collection, analyses, or interpretation of data; in the writing of the manuscript; or in the decision to publish the results.

## Appendix A

The formulas estimating the status of EMT, glioma, glioma stem cells, molecular target therapy genes, and potential glioma biomarkers based on the Cox proportional hazard regression analysis.

### [TCGA and CGGA data sets]

Epithelial markers:  $0.229 \text{ CLDN1} + 0.203 \text{ DSG3}$

Mesenchymal markers:  $0.581 \text{ FN1} - 0.411 \text{ CDH11}$

Glioma markers:  $0.529 \text{ HDAC7} - 0.64 \text{ HDAC1} + 0.404 \text{ MGMT} - 0.627 \text{ PTEN} + 0.639 \text{ HDAC3} - 0.306 \text{ EGFR} - 0.33 \text{ PGF} + 0.424 \text{ FLT1}$

Glioma stem cell markers:  $0.388 \text{ L1CAM} - 0.267 \text{ OLIG2} + 0.401 \text{ STAT3} - 0.307 \text{ BMI1}$

Molecular target therapy genes:  $0.61 \text{ HDAC7} - 0.559 \text{ HDAC1} + 0.639 \text{ HDAC3} - 0.34 \text{ SIRT1} - 0.229 \text{ EGFR}$

Potential glioma biomarkers:  $0.548 \text{ IGFBP2} - 0.634 \text{ TIMP4} + 0.482 \text{ GFAP} + 0.335 \text{ MGMT} - 0.369 \text{ GADD45A} + 0.212 \text{ MMP9}$

## Appendix B

The formulas estimating the status of EMT, glioma, glioma stem cells, molecular target therapy, and potential glioma biomarkers based on the principal component analysis.

### [TCGA data set]

Epithelial markers:  $0.134 \text{ CDH1} + 0.29 \text{ CLDN1} + 0.401 \text{ COL4A1} + 0.035 \text{ DSC1} + 0.048 \text{ DSG3} + 0.36 \text{ DSP} + 0.123 \text{ KRT1} + 0.35 \text{ KRT18} + 0.113 \text{ LAMA1} + 0.284 \text{ MUC1} + 0.421 \text{ NID1} + 0.305 \text{ SDC1} + 0.321 \text{ TJP1}$

Mesenchymal markers:  $0.224 \text{ ACTA2} + 0.259 \text{ CDH11} + 0.19 \text{ CDH2} + 0.235 \text{ COL1A1} + 0.227 \text{ COL3A1} + 0.21 \text{ CTNNA1} + 0.215 \text{ ETS1} + 0.268 \text{ FN1} + 0.21 \text{ FOXC2} + 0.126 \text{ GSC} + 0.28 \text{ ITGA5} + 0.203 \text{ ITGAV} + 0.284 \text{ ITGB1} + 0.063 \text{ ITGB6} + 0.192 \text{ LAMA5} + 0.216 \text{ LEF1} + 0.215 \text{ RUNX2} + 0.152 \text{ S100A4} + 0.174 \text{ SNAI1} + 0.205 \text{ SNAI2} + 0.135 \text{ TWIST1} + 0.23 \text{ VIM} + 0.125 \text{ ZEB1}$

Glioma markers:  $0.156 \text{ ATRX} + 0.167 \text{ BRAF} + 0.062 \text{ CDK4} + 0.037 \text{ CDKN2A} + 0.122 \text{ H3F3A} + 0.14 \text{ HIF1A} + 0.044 \text{ MET} + 0.161 \text{ NF1} + 0.166 \text{ PIK3CA} + 0.179 \text{ PIK3CB} + 0.108 \text{ PIK3CG} + 0.147 \text{ PTEN} + 0.125 \text{ RB1} + 0.072 \text{ TERT} + 0.151 \text{ TP53} + 0.057 \text{ PTGS2} + 0.098 \text{ DEPTOR} + 0.067 \text{ EGFR} + 0.142 \text{ FLT1} + 0.12 \text{ FLT4} + 0.17 \text{ HDAC1} + 0.144 \text{ HDAC10} + 0.145 \text{ HDAC11} + 0.135 \text{ HDAC2} + 0.176 \text{ HDAC3} + 0.173 \text{ HDAC4} + 0.173 \text{ HDAC5} + 0.18 \text{ HDAC6} + 0.15 \text{ HDAC7} + 0.183 \text{ HDAC8} + 0.157 \text{ HDAC9} + 0.135 \text{ KDR} + 0.162 \text{ MLST8} + 0.174 \text{ MTOR} + 0.053 \text{ PDGFRA} + 0.038 \text{ PGF} + 0.148 \text{ RICTOR} + 0.178 \text{ RPTOR} + 0.173 \text{ SIRT1} + 0.105 \text{ SIRT2} + 0.168 \text{ SIRT3} + 0.133 \text{ SIRT4} + 0.173 \text{ SIRT5} + 0.169 \text{ SIRT6} + 0.184 \text{ SIRT7} + 0.082 \text{ VEGFA} + 0.151 \text{ VEGFB} + 0.078 \text{ VEGFC} + 0.069 \text{ VEGFD} + 0.027 \text{ CHI3L1} + 0.137 \text{ IDH1} + 0.154 \text{ IDH2} + 0.061 \text{ MGMT}$

Glioma stem cell markers:  $0.251 \text{ BMI1} + 0.243 \text{ CD44} + 0.263 \text{ FUT4} + 0.298 \text{ ITGA6} + 0.249 \text{ KLF4} + 0.16 \text{ L1CAM} + 0.32 \text{ MSI1} + 0.207 \text{ MYC} + 0.176 \text{ NANOG} + 0.269 \text{ NES} + 0.204 \text{ OLIG2} + 0.129 \text{ POU5F1} + 0.15 \text{ PROM1} + 0.134 \text{ SALL4} + 0.307 \text{ SOX2} + 0.346 \text{ STAT3} + 0.266 \text{ GFAP}$

Molecular target therapy genes: 0.063 PTGS2 + 0.114 DEPTOR + 0.072 EGFR + 0.166 FLT1 + 0.147 FLT4 + 0.202 HDAC1 + 0.178 HDAC10 + 0.181 HDAC11 + 0.158 HDAC2 + 0.204 HDAC3 + 0.207 HDAC4 + 0.214 HDAC5 + 0.217 HDAC6 + 0.18 HDAC7 + 0.216 HDAC8 + 0.179 HDAC9 + 0.157 KDR + 0.197 MLST8 + 0.204 MTOR + 0.062 PDGFRA + 0.054 PGF + 0.176 RICTOR + 0.214 RPTOR + 0.2 SIRT1 + 0.131 SIRT2 + 0.202 SIRT3 + 0.161 SIRT4 + 0.207 SIRT5 + 0.208 SIRT6 + 0.225 SIRT7 + 0.097 VEGFA + 0.185 VEGFB + 0.095 VEGFC + 0.089 VEGFD

Potential glioma biomarkers: 0.028 AHSG + 0.281 CD63 + 0.22 CHI3L1 + 0.178 FABP5 + 0.08 FOXM1 + 0.199 FSTL1 + 0.267 GADD45A + 0.17 GFAP + 0.193 GSN + 0.248 IDH1 + 0.181 IDH2 + 0.175 IGFBP2 + 0.268 IQGAP1 + 0.166 MGMT + 0.112 MMP9 + 0.254 NAMPT + 0.178 PEA15 + 0.175 PTPRZ1 + 0.253 S100A10 + 0.27 S100A6 + 0.215 SPP1 + 0.179 STARD13 + 0.253 TBCA + 0.119 TIMP4

#### [CGGA data set]

Epithelial markers:  $-0.15$  CDH1 +  $0.361$  CLDN1 +  $0.502$  COL4A1  $-0.049$  DSC1 +  $0.132$  DSG3 +  $0.328$  DSP +  $0.206$  KRT1 +  $0.343$  KRT18 +  $0.221$  LAMA1 +  $0.072$  MUC1 +  $0.479$  NID1 +  $0.153$  SDC1  $-0.038$  TJP1

Mesenchymal markers:  $-0.263$  ACTA2  $-0.23$  CDH11  $-0.116$  CDH2  $-0.308$  COL1A1  $-0.313$  COL3A1  $-0.092$  CTNNB1  $-0.144$  ETS1  $-0.295$  FN1  $-0.261$  FOXC2  $-0.085$  GSC  $-0.313$  ITGA5  $-0.067$  ITGAV  $-0.218$  ITGB1  $-0.15$  LAMA5  $-0.16$  LEF1  $-0.149$  RUNX2  $-0.214$  S100A4  $-0.24$  SNAI1  $-0.29$  SNAI2  $-0.17$  TWIST1  $-0.21$  VIM +  $0.007$  ZEB1

Glioma markers:  $0.205$  ATRX +  $0.249$  BRAF +  $0.022$  CDK4  $-0.043$  CDKN2A +  $0.087$  H3F3A +  $0.041$  HIF1A +  $0.059$  MET +  $0.233$  NF1 +  $0.225$  PIK3CA +  $0.261$  PIK3CB +  $0.08$  PIK3CG +  $0.082$  PTEN +  $0.097$  RB1  $-0.028$  TERT +  $0.124$  TP53  $-0.058$  PTGS2 +  $0.132$  DEPTOR +  $0.088$  EGFR  $-0.021$  FLT1  $-0.134$  FLT4  $-0.182$  HDAC1  $-0.081$  HDAC10 +  $0.15$  HDAC11 +  $0.089$  HDAC2  $-0.09$  HDAC3 +  $0.125$  HDAC4 +  $0.258$  HDAC5 +  $0.047$  HDAC6 +  $0.007$  HDAC7  $-0.149$  HDAC8 +  $0.114$  HDAC9  $-0.002$  KDR +  $0.153$  MLST8 +  $0.205$  MTOR +  $0.145$  PDGFRA  $-0.092$  PGF +  $0.246$  RPTOR +  $0.242$  SIRT1 +  $0.17$  SIRT2 +  $0.05$  SIRT3 +  $0.012$  SIRT4  $-0.086$  SIRT5  $-0.128$  SIRT6  $-0.165$  SIRT7  $-0.063$  VEGFB  $-0.123$  VEGFC  $-0.003$  VEGFD  $-0.19$  CHI3L1 +  $0.164$  IDH1  $-0.018$  IDH2  $-0.213$  MGMT

Glioma stem cell markers:  $0.323$  BMI1  $-0.381$  CD44  $-0.342$  FUT4  $-0.103$  ITGA6  $-0.281$  KLF4 +  $0.053$  L1CAM +  $0.329$  MSI1 +  $0.003$  MYC +  $0.159$  NANOG  $-0.071$  NES +  $0.373$  OLIG2 +  $0.002$  POU5F1  $-0.015$  PROM1  $-0.184$  SALL4 +  $0.409$  SOX2  $-0.23$  STAT3 +  $0.099$  GFAP

Molecular target therapy genes:  $-0.163$  PTGS2 +  $0.197$  DEPTOR +  $0.056$  EGFR  $-0.153$  FLT1  $-0.221$  FLT4  $-0.249$  HDAC1  $-0.109$  HDAC10 +  $0.259$  HDAC11 +  $0.111$  HDAC2  $-0.199$  HDAC3 +  $0.215$  HDAC4 +  $0.323$  HDAC5 +  $0.104$  HDAC6  $-0.095$  HDAC7  $-0.174$  HDAC8 +  $0.115$  HDAC9  $-0.113$  KDR +  $0.18$  MLST8 +  $0.202$  MTOR +  $0.173$  PDGFRA  $-0.127$  PGF +  $0.246$  RPTOR +  $0.277$  SIRT1 +  $0.252$  SIRT2 +  $0.108$  SIRT3 +  $0.04$  SIRT4  $-0.115$  SIRT5  $-0.109$  SIRT6  $-0.169$  SIRT7  $-0.07$  VEGFB  $-0.222$  VEGFC  $-0.012$  VEGFD

Potential glioma biomarkers:  $0.056$  AHSG  $-0.272$  CD63  $-0.328$  CHI3L1  $-0.281$  FABP5 +  $0.073$  FOXM1  $-0.283$  FSTL1  $-0.215$  GADD45A +  $0.045$  GFAP  $-0.028$  GSN  $-0.021$  IDH1 +  $0.036$  IDH2  $-0.258$  IGFBP2  $-0.287$  IQGAP1  $-0.159$  MGMT  $-0.248$  MMP9  $-0.302$  NAMPT +  $0.19$  PEA15 +  $0.154$  PTPRZ1  $-0.286$  S100A10  $-0.251$  S100A6  $-0.224$  SPP1 +  $0.047$  STARD13  $-0.116$  TBCA +  $0.05$  TIMP4

#### Appendix C

The formulas estimating the combined statuses of EMT, glioma, glioma stem cells, and potential glioma biomarkers based on the Cox proportional hazard regression analysis.

Combinatorial equation for status:  $0.229$  CLDN1 +  $0.203$  DSG3 +  $0.581$  FN1  $-0.411$  CDH11 +  $0.529$  HDAC7 +  $0.639$  HDAC3  $-0.627$  PTEN +  $0.388$  L1CAM  $-0.267$  OLIG2 +  $0.548$  IGFBP2  $-0.634$  TIMP4  $-0.369$  GADD45A

## References

1. Louis, D.N.; Perry, A.; Reifenberger, G.; von Deimling, A.; Figarella-Branger, D.; Cavenee, W.K.; Ohgaki, H.; Wiestler, O.D.; Kleihues, P.; Ellison, D.W. The 2016 World Health Organization Classification of Tumors of the Central Nervous System: A summary. *Acta Neuropathol.* **2016**, *131*, 803–820. [[CrossRef](#)] [[PubMed](#)]
2. Silantyev, A.S.; Falzone, L.; Libra, M.; Gurina, O.I.; Kardashova, K.S.; Nikolouzakakis, T.K.; Nosyrev, A.E.; Sutton, C.W.; Mitsias, P.D.; Tsatsakis, A. Current and Future Trends on Diagnosis and Prognosis of Glioblastoma: From Molecular Biology to Proteomics. *Cells* **2019**, *8*, 863. [[CrossRef](#)] [[PubMed](#)]
3. Stewart, L.A. Chemotherapy in adult high-grade glioma: A systematic review and meta-analysis of individual patient data from 12 randomised trials. *Lancet* **2002**, *359*, 1011–1018. [[PubMed](#)]
4. Stupp, R.; Hegi, M.E.; Mason, W.P.; van den Bent, M.J.; Taphoorn, M.J.; Janzer, R.C.; Ludwin, S.K.; Allgeier, A.; Fisher, B.; Belanger, K.; et al. Effects of radiotherapy with concomitant and adjuvant temozolomide versus radiotherapy alone on survival in glioblastoma in a randomised phase III study: 5-year analysis of the EORTC-NCIC trial. *Lancet Oncol.* **2009**, *10*, 459–466. [[CrossRef](#)]
5. Tran, B.; Rosenthal, M.A. Survival comparison between glioblastoma multiforme and other incurable cancers. *J. Clin. Neurosci.* **2010**, *17*, 417–421. [[CrossRef](#)]
6. Iser, I.C.; Pereira, M.B.; Lenz, G.; Wink, M.R. The Epithelial-to-Mesenchymal Transition-Like Process in Glioblastoma: An Updated Systematic Review and In Silico Investigation. *Med. Res. Rev.* **2017**, *37*, 271–313. [[CrossRef](#)] [[PubMed](#)]
7. Rajesh, Y.; Biswas, A.; Mandal, M. Glioma progression through the prism of heat shock protein mediated extracellular matrix remodeling and epithelial to mesenchymal transition. *Exp. Cell Res.* **2017**, *359*, 299–311. [[CrossRef](#)]
8. Li, L.; Wu, M.; Wang, C.; Yu, Z.; Wang, H.; Qi, H.; Xu, X.  $\beta$ -Asarone Inhibits Invasion and EMT in Human Glioma U251 Cells by Suppressing Splicing Factor HnRNP A2/B1. *Molecules* **2018**, *23*, 671. [[CrossRef](#)]
9. Wu, H.; Li, X.; Feng, M.; Yao, L.; Deng, Z.; Zao, G.; Zhou, Y.; Chen, S.; Du, Z. Downregulation of RNF138 inhibits cellular proliferation, migration, invasion and EMT in glioma cells via suppression of the Erk signaling pathway. *Oncol. Rep.* **2018**, *40*, 3285–3296. [[CrossRef](#)]
10. Iwate, Y. Epithelial-mesenchymal transition in glioblastoma progression. *Oncol. Lett.* **2016**, *11*, 1615–1620. [[CrossRef](#)]
11. Lee, J.M.; Dedhar, S.; Kalluri, R.; Thompson, E.W. The epithelial-mesenchymal transition: New insights in signaling, development, and disease. *J. Cell Biol.* **2006**, *172*, 973–981. [[CrossRef](#)] [[PubMed](#)]
12. Kalluri, R.; Weinberg, R.A. The basics of epithelial-mesenchymal transition. *J. Clin. Invest.* **2009**, *119*, 1420–1428. [[CrossRef](#)] [[PubMed](#)]
13. Iwate, Y. Plasticity in Glioma Stem Cell Phenotype and Its Therapeutic Implication. *Neurol. Med. Chir.* **2018**, *58*, 61–70. [[CrossRef](#)] [[PubMed](#)]
14. Takahashi, K.; Yamanaka, S. Induction of pluripotent stem cells from mouse embryonic and adult fibroblast cultures by defined factors. *Cell* **2006**, *126*, 663–676. [[CrossRef](#)] [[PubMed](#)]
15. Yu, J.; Vodyanik, M.A.; Smuga-Otto, K.; Antosiewicz-Bourget, J.; Frane, J.L.; Tian, S.; Nie, J.; Jonsdottir, G.A.; Ruotti, V.; Stewart, R.; et al. Induced pluripotent stem cell lines derived from human somatic cells. *Science* **2007**, *318*, 1917–1920. [[CrossRef](#)]
16. Hattermann, K.; Flüh, C.; Engel, D.; Mehdorn, H.M.; Synowitz, M.; Mentlein, R.; Held-Feindt, J. Stem cell markers in glioma progression and recurrence. *Int. J. Oncol.* **2016**, *49*, 1899–1910. [[CrossRef](#)]
17. Lv, D.; Ma, Q.H.; Duan, J.J.; Wu, H.B.; Zhao, X.L.; Yu, S.C.; Bian, X.W. Optimized dissociation protocol for isolating human glioma stem cells from tumorspheres via fluorescence-activated cell sorting. *Cancer Lett.* **2016**, *377*, 105–115. [[CrossRef](#)]
18. Colquhoun, A. Cell biology-metabolic crosstalk in glioma. *Int. J. Biochem. Cell. Biol.* **2017**, *89*, 171–181. [[CrossRef](#)]
19. Takashima, Y.; Kawaguchi, A.; Kanayama, T.; Hayano, A.; Yamanaka, R. Correlation between lower balance of Th2 helper T-cells and expression of PD-L1/PD-1 axis genes enables prognostic prediction in patients with glioblastoma. *Oncotarget* **2018**, *9*, 19065–19078. [[CrossRef](#)]
20. Takashima, Y.; Kawaguchi, A.; Hayano, A.; Yamanaka, R. CD276 and the gene signature composed of GATA3 and LGALS3 enable prognosis prediction of glioblastoma multiforme. *PLoS ONE* **2019**, *14*, e0216825. [[CrossRef](#)]

21. Ashburner, M.; Ball, C.A.; Blake, J.A.; Botstein, D.; Butler, H.; Cherry, J.M.; Davis, A.P.; Dolinski, K.; Dwight, S.S.; Eppig, J.T.; et al. Gene ontology: Tool for the unification of biology. The Gene Ontology Consortium. *Nat. Genet.* **2000**, *25*, 25–29. [[CrossRef](#)] [[PubMed](#)]
22. Dennis, G., Jr.; Sherman, B.T.; Hosack, D.A.; Yang, J.; Gao, W.; Lane, H.C.; Lempicki, R.A. DAVID: Database for Annotation, Visualization, and Integrated Discovery. *Genome Biol.* **2003**, *4*, 3. [[CrossRef](#)]
23. Takashima, Y.; Sasaki, Y.; Hayano, A.; Homma, J.; Fukai, J.; Iwate, Y.; Kajiwara, K.; Ishizawa, S.; Hondoh, H.; Tokino, T.; et al. Target amplicon exome-sequencing identifies promising diagnosis and prognostic markers involved in RTK-RAS and PI3K-AKT signaling as central oncopathways in primary central nervous system lymphoma. *Oncotarget* **2018**, *9*, 27471–27486. [[CrossRef](#)] [[PubMed](#)]
24. Ishwaran, H.; Kogalur, U.B.; Blackstone, E.H.; Lauer, M.S. Random survival forests. *Ann. Appl. Stat.* **2008**, *2*, 841–860. [[CrossRef](#)]
25. Kawaguchi, A.; Iwate, Y.; Komohara, Y.; Sano, M.; Kajiwara, K.; Yajima, N.; Tsuchiya, N.; Homma, J.; Aoki, H.; Kobayashi, T.; et al. Gene expression signature-based prognostic risk score in patients with primary central nervous system lymphoma. *Clin. Cancer Res.* **2012**, *18*, 5672–5681. [[CrossRef](#)]
26. Kawaguchi, A.; Yajima, N.; Tsuchiya, N.; Homma, J.; Sano, M.; Natsumeda, M.; Takahashi, H.; Fujii, Y.; Kakuma, T.; Yamanaka, R. Gene expression signature-based prognostic risk score in patients with glioblastoma. *Cancer Sci.* **2013**, *104*, 1205–1210. [[CrossRef](#)]
27. Takashima, Y.; Kawaguchi, A.; Sato, R.; Yoshida, K.; Hayano, A.; Homma, J.; Fukai, J.; Iwate, Y.; Kajiwara, K.; Ishizawa, S.; et al. Differential expression of individual transcript variants of PD-1 and PD-L2 genes on Th-1/Th-2 status is guaranteed for prognosis prediction in PCNSL. *Sci. Rep.* **2019**, *9*, 10004. [[CrossRef](#)]
28. Meinshausen, N.; Bühlmann, P. High dimensional graphs and variable selection with the lasso. *Ann. Stat.* **2006**, *34*, 1436–1462. [[CrossRef](#)]
29. Friedman, J.; Hastie, T.; Tibshirani, R. Sparse inverse covariance estimation with the graphical lasso. *Biostatistics* **2008**, *9*, 432–441. [[CrossRef](#)]
30. Leblanc, M.; Crowley, J. Survival trees by goodness of split. *J. Am. Stat. Assoc.* **1993**, *88*, 457–467. [[CrossRef](#)]
31. Nishida, Y.; Kimura, S.; Mizobe, H.; Yamamichi, J.; Kojima, K.; Kawaguchi, A.; Fujisawa, M.; Matsue, K. Automatic digital quantification of bone marrow myeloma volume in appendicular skeletons—clinical implications and prognostic significance. *Sci. Rep.* **2017**, *7*, 12885. [[CrossRef](#)] [[PubMed](#)]
32. R Development Core Team. *R: A Language and Environment for Statistical Computing*; R Foundation for Statistical Computing: Vienna, Austria, 2011.
33. Gentleman, R.C.; Carey, V.J.; Bates, D.M.; Bolstad, B.; Dettling, M.; Dudoit, S.; Ellis, B.; Gautier, L.; Ge, Y.; Gentry, J.; et al. Bioconductor: Open software development for computational biology and bioinformatics. *Genome Biol.* **2004**, *5*, 80. [[CrossRef](#)] [[PubMed](#)]
34. Zeisberg, M.; Neilson, E.G. Biomarkers for epithelial-mesenchymal transitions. *J. Clin. Invest.* **2009**, *119*, 1429–1437. [[CrossRef](#)] [[PubMed](#)]
35. Liang, S.; Shen, G. Biomarkers of Glioma. In *Molecular Targets of CNS Tumors*; Garami, M., Ed.; N InTech Europe: London, UK, 2011; p. 325.
36. Otani, R.; Uzuka, T.; Ueki, K. Classification of adult diffuse gliomas by molecular markers—a short review with historical footnote. *Jpn. J. Clin. Oncol.* **2017**, *47*, 2–6. [[CrossRef](#)] [[PubMed](#)]
37. Ludwig, K.; Kornblum, H.I. Molecular markers in glioma. *J. Neurooncol.* **2017**, *134*, 505–512. [[CrossRef](#)]
38. Jhaveri, N.; Chen, T.C.; Hofman, F.M. Tumor vasculature and glioma stem cells: Contributions to glioma progression. *Cancer Lett.* **2016**, *380*, 545–551. [[CrossRef](#)]
39. Pradella, D.; Naro, C.; Sette, C.; Ghigna, C. EMT and stemness: Flexible processes tuned by alternative splicing in development and cancer progression. *Mol. Cancer* **2017**, *16*, 8. [[CrossRef](#)]
40. Quezada, C.; Torres, Á.; Niechi, I.; Uribe, D.; Contreras-Duarte, S.; Toledo, F.; San Martín, R.; Gutiérrez, J.; Sobrevia, L. Role of extracellular vesicles in glioma progression. *Mol. Aspects Med.* **2018**, *60*, 38–51. [[CrossRef](#)]
41. Wang, S.; Yao, F.; Lu, X.; Li, Q.; Su, Z.; Lee, J.H.; Wang, C.; Du, L. Temozolomide promotes immune escape of GBM cells via upregulating PD-L1. *Am. J. Cancer Res.* **2019**, *9*, 1161–1171.
42. Kloosterman, W.P.; Coebergh van den Braak, R.R.J.; Pieterse, M.; van Roosmalen, M.J.; Sieuwerts, A.M.; Stangl, C.; Brunekreef, R.; Lalmahomed, Z.S.; Ooft, S.; van Galen, A.; et al. A Systematic Analysis of Oncogenic Gene Fusions in Primary Colon Cancer. *Cancer Res.* **2017**, *77*, 3814–3822. [[CrossRef](#)]
43. Kim, R.N.; Moon, H.G.; Han, W.; Noh, D.Y. Perspective Insight into Future Potential Fusion Gene Transcript Biomarker Candidates in Breast Cancer. *Int. J. Mol. Sci.* **2018**, *19*, 502. [[CrossRef](#)] [[PubMed](#)]

44. Nduom, E.K.; Wei, J.; Yaghi, N.K.; Huang, N.; Kong, L.Y.; Gabrusiewicz, K.; Ling, X.; Zhou, S.; Ivan, C.; Chen, J.Q.; et al. PD-L1 expression and prognostic impact in glioblastoma. *Neuro Oncol.* **2016**, *18*, 195–205. [[CrossRef](#)] [[PubMed](#)]
45. Wang, Z.; Zhang, C.; Liu, X.; Wang, Z.; Sun, L.; Li, G.; Liang, J.; Hu, H.; Liu, Y.; Zhang, W.; et al. Molecular and clinical characterization of PD-L1 expression at transcriptional level via 976 samples of brain glioma. *Oncoimmunology* **2016**, *5*, e1196310. [[CrossRef](#)] [[PubMed](#)]
46. Allen, E.; Jabouille, A.; Rivera, L.B.; Lodewijckx, I.; Missiaen, R.; Steri, V.; Feyen, K.; Tawney, J.; Hanahan, D.; Michael, I.P.; et al. Combined antiangiogenic and anti-PD-L1 therapy stimulates tumor immunity through HEV formation. *Sci. Transl. Med.* **2017**, *9*, 9679. [[CrossRef](#)]
47. Koekkoek, J.A.; Dirven, L.; Heimans, J.J.; Postma, T.J.; Vos, M.J.; Reijneveld, J.C.; Taphoorn, M.J. Seizure reduction in a low-grade glioma: More than a beneficial side effect of temozolomide. *J. Neurol. Neurosurg. Psychiatry* **2015**, *86*, 366–373. [[CrossRef](#)]
48. Chio, C.C.; Chen, K.Y.; Chang, C.K.; Chuang, J.Y.; Liu, C.C.; Liu, S.H.; Chen, R.M. Improved effects of honokiol on temozolomide-induced autophagy and apoptosis of drug-sensitive and -tolerant glioma cells. *BMC Cancer* **2018**, *18*, 379. [[CrossRef](#)]
49. Tsuchiya, N.; Yamanaka, R.; Yajima, N.; Homma, J.; Sano, M.; Komata, T.; Ikeda, T.; Fujimoto, I.; Takahashi, H.; Tanaka, R.; et al. Isolation and characterization of an N-linked oligosaccharide that is increased in glioblastoma tissue and cell lines. *Int. J. Oncol.* **2005**, *27*, 1231–1239. [[CrossRef](#)]
50. Takashima, Y.; Yoshimura, T.; Kano, Y.; Hayano, A.; Hondoh, H.; Ikenaka, K.; Yamanaka, R. Differential expression of N-linked oligosaccharides in methotrexate-resistant primary central nervous system lymphoma cells. *BMC Cancer* **2019**, *19*, 910. [[CrossRef](#)]
51. Hayano, A.; Komohara, Y.; Takashima, Y.; Takeya, H.; Homma, J.; Fukai, J.; Iwadate, Y.; Kajiwara, K.; Ishizawa, S.; Hondoh, H.; et al. Programmed Cell Death Ligand 1 Expression in Primary Central Nervous System Lymphomas: A Clinicopathological Study. *Anticancer Res.* **2017**, *37*, 5655–5666.
52. Miyasato, Y.; Takashima, Y.; Takeya, H.; Yano, H.; Hayano, A.; Nakagawa, T.; Makino, K.; Takeya, M.; Yamanaka, R.; Komohara, Y. The expression of PD-1 ligands and IDO1 by macrophage/microglia in primary central nervous system lymphoma. *J. Clin. Exp. Hematop.* **2018**, *58*, 95–101. [[CrossRef](#)]
53. Takashima, Y.; Kawaguchi, A.; Iwadate, Y.; Hondoh, H.; Fukai, J.; Kajiwara, K.; Hayano, A.; Yamanaka, R. MicroRNA signature constituted of miR-30d, miR-93, and miR-181b is a promising prognostic marker in primary central nervous system lymphoma. *PLoS ONE* **2019**, *14*, e0210400. [[CrossRef](#)] [[PubMed](#)]



© 2019 by the authors. Licensee MDPI, Basel, Switzerland. This article is an open access article distributed under the terms and conditions of the Creative Commons Attribution (CC BY) license (<http://creativecommons.org/licenses/by/4.0/>).